



Imaging Subsurface Structures at Fast Eroding Coastal Areas in Northern Bengkulu Using 2D Seismic MASW Method

Ashar Muda Lubis¹ · Rida Samdara¹ · Lita Angraini² · Zia Ahmed^{3,4} · Dominic E. Reeve⁵

Received: 20 August 2021 / Revised: 16 February 2022 / Accepted: 17 February 2022 / Published online: 8 March 2022
© King Abdulaziz University and Springer Nature Switzerland AG 2022

Abstract

Coastal erosion is a global problem, affecting many countries around the world. On cliffed coastlines, erosion can be intermittent and sudden, posing an additional hazard to coastal communities. To mitigate such problems, it is necessary to understand the processes leading to cliff erosion. Here, we focus on the physical properties of the subsurface structure that might contribute to cliff instability. As a specific study site, we use the coastal region of the northern part of Bengkulu Province, which is well known as being prone to coastal abrasion/erosion. Seismic field surveys were conducted at five locations, using a 92 m seismic line with geophones spaced every 2 m. The measurements were processed using the Multichannel Analysis of Surface Wave (MASW) methodology with commercially available software. Our results suggest that the subsurfaces are divided into three layers where the top layers lie at thickness between 10 and 15 m with S-wave velocity (V_s) < 200 m/s (consistent with diluvial clay). The second layer has a thickness > 10 m with V_s between 600 and 800 m/s (consistent with loose sand), and overlays a bedrock layer for which V_s is much higher. We found between the first and second layers are a narrow ‘discontinuity region’ with V_s of 300–500 m/s (consistent with soft sand/silt). The configuration/composition/orientation of layers indicate stable permeable layers overlying saturated and impermeable layers at or below the sea level. The upper permeable layers are vulnerable to instability when subjected to external disturbances such as heavy precipitation, storm waves or earthquakes. The relatively mild wave climate and absence of notching around the water line leads us to conclude that variation in saturation levels is the primary driver of the observed cliff erosion.

Keywords Coastal · Abrasion · Subsurface structure · S-wave velocity

1 Introduction

Coastal erosion is a global problem, affecting many countries around the world. Over the last decade, most of the coastal areas of Bengkulu Province, Indonesia have suffered from erosion, experiencing very extensive coastal abrasion, up to 20 m/year in the northern part of Bengkulu Province. In general, the shorelines regions of northern Bengkulu have a very steep topography and are very vulnerable to coastal erosion. Several villages in the north of the Bengkulu region have been lost to the sea due to coastal abrasion/erosion. Furthermore, cliffed coastal abrasion has damaged vital transport infrastructure such as roads and bridges, as well as conurbations and commercial centres, affecting the social-economic life of the regional communities. To mitigate such problems, it is necessary to understand the processes leading to cliff erosion.

In general, coastal erosion can be caused by changes in natural phenomena, (such as increased storminess, sea level

✉ Ashar Muda Lubis
asharml@unib.ac.id

¹ Department of Physics, Faculty of Mathematics and Natural Sciences, University of Bengkulu, Jl. WR Supratman, Kadang Limun, Bengkulu 38371, Indonesia

² Kepahiang Geophysics Station, Meteorological, Climatological, and Geophysical Agency of Indonesia, Jl. Pembangunan, Kepahiang, Bengkulu, Indonesia

³ Department of Geosciences, Mississippi State University, MS-39762, Mississippi State, USA

⁴ Department of Geography and Environment, Shahjalal University of Science and Technology, Sylhet 3114, Bangladesh

⁵ Coastal Engineering Research Group, Zienkiewicz Centre for Computational Engineering, Swansea University, Bay Campus, Swansea SA1 8EN, Wales, UK

rise, prolonged intense rainfall), and by anthropogenic interventions that disrupt the movement of material along the shore, (e.g. Mimura 2013; Toimil et al. 2020). The consequences, with specific focus on developing countries, were highlighted by Nicholls and Leatherman (1995). The publication of the Intergovernmental Panel on Climate Change, the 4th Assessment Report (IPCC 2007) was a significant milestone in several respects. First, there was more evidence of links between the physical processes and changes in climate; second, there were further observations of increasing temperatures, retreat of ice sheets, and rising global mean sea level; and third, there was evidence to support increased confidence that the frequency of extreme weather events would increase in some regions and thereby affect coastal erosion. Significantly, there was a recognition that while most attention had been directed towards the effects of sea-level rise and consequent flood threat, coastal erosion was another separate coastal impact that deserved attention and required projections of additional information such as waves and surges, as noted by Hemer et al. (2013). This had been recognized by Dickson et al. (2007) in their assessment of climate change on cliff erosion which included the effects of sea level rise and wave action, but excluded rainfall effects.

After a cliff fall, the fallen material can be washed along-shore and removed by strong backwash from the beach; the preferred mechanism is strongly controlled by wave heights and breaking wave incidence angles (Ashton and Murray 2006; Türker and Kabdaşlı 2006; Warrick et al. 2019). Nevertheless, the process of cliff erosion is influenced by the strength of the subsurface geological structure and their exposure in the coastal region. Therefore, further

understanding of the physical properties of the subsurface structure in coastal regions is very important in assessing their response to changes in physical erosion processes. In this study, we investigated the subsurface structure at five foreshore regions/villages in the northern part of Bengkulu where the rate of shoreline erosion is relatively very high, with the aim of providing new insights into how the erosion in northern Bengkulu is affected by geological factors.

In Sect. 2, a brief description of the study site is given. The methods used are presented in Sect. 3, with results shown in Sect. 4. The paper ends with Conclusions in Sect. 5. Such kind of study has been intensively used in other regions (e.g. Miller 2016; Rehman et al. 2016; Chandran and Anbazhagan 2017; Hussain et al. 2019; Keskinsezer and Dağ 2019; Eccleston and Spyrou 2019; Owoc et al. 2019; Daryono et al. 2020). To achieve our goal, we employed a seismic active Multichannel Analysis of Surface Wave (MASW) method during field works seismic surveys.

2 Study Site

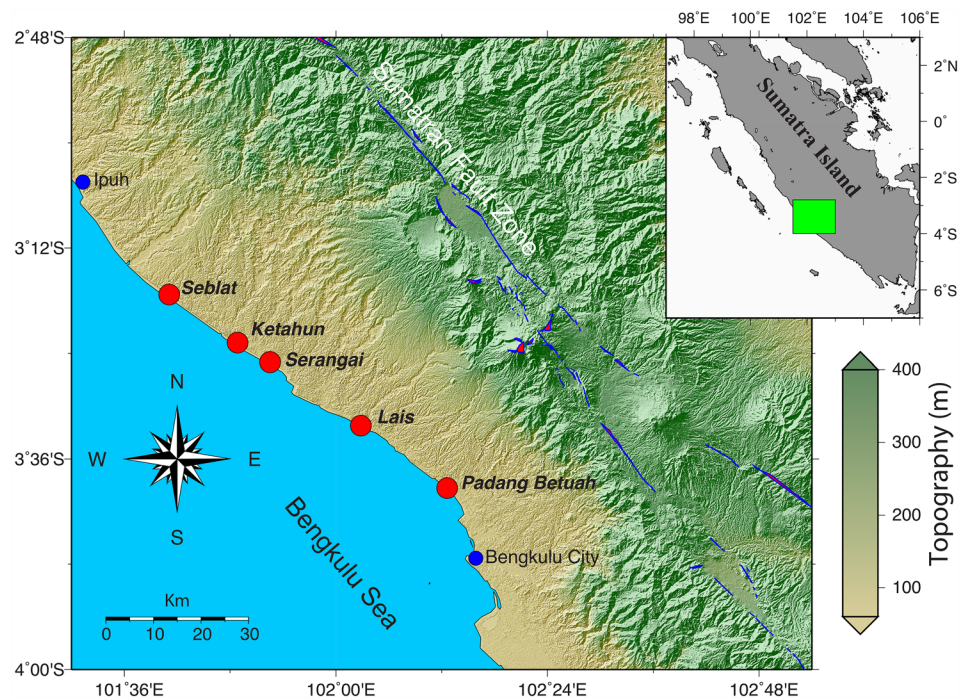
The study site is Bengkulu. It is a province in Indonesia and is located on the southwest of Sumatra. Figure 1 shows a location map.

Bengkulu has an annual rainfall of 2900–3600 mm, and the mean annual temperature is 25–32 °C (Supriyono et al. 2021). Based on these weather conditions, Bengkulu is classified as being ‘wet tropical’ with a humidity of 70–87% (Case et al. 2007). Moreover, according to Paski et al. (2021), North Bengkulu and the Central area of the



Fig. 1 Map showing location of Bengkulu within Indonesian archipelago

Fig. 2 Location of seismic surveys at foreshore regions in the north part of Bengkulu. Five sites of seismic surveys at foreshore areas in the northern part of Bengkulu (red cycles), at Padang Betuah, Lais, Serangai, Ketahun and Seblat areas from south to north. The inset map is Sumatra Island which showing a research area map (green rectangular)



Bengkulu Province have a heavy rainfall distribution, which may contribute to coastal cliff instability.

In the northern Bengkulu regions, Samdara (2014) has examined sea level variation using satellite altimetry data from 1994 to 2013. The results showed that the rate of sea-level change is relatively low compared to the global sea-level change of 3.8 ± 0.3 mm/year since the end of twentieth century (Wang et al. 2021). Additionally, the rate of change in sea-level in Bengkulu does not seem to be linearly correlated with the abrasion rate (Samdara 2014). Therefore, it can be assumed that the sea-level change factor is not the main cause of coastal abrasion in the northern part of Bengkulu.

Furthermore, the tectonic activities related to co-seismic and post-seismic deformations associated with large earthquakes and inter-seismic process can cause land surface changes (Lubis et al. 2011, 2013) and inducing coastal erosion. In coastal areas, deformations related to tectonic activities reach also uplift or subsidence coastal regions, causing shoreline changes. Fortunately, there is no large earthquake and tsunami occurring in the northern part of Bengkulu in the last decade. Hence, vertical coastal changes associated with co-seismic and post-seismic deformations may have insignificant effect to coastal erosion in last past 10 years.

3 Methods

We employed a seismic active Multichannel Analysis of Surface Wave (MASW) method during field works seismic surveys. Such kind of study has been intensively used in other regions (e.g. Miller 2016; Keskinsezer and Dağ 2019; Eccleston and Spyrou 2019; Daryono et al. 2020). To achieve our goal, we employed a seismic active Multichannel Analysis of Surface Wave (MASW) method during field works seismic surveys.

The MASW method was first introduced by Park et al. (1999), and it is very powerful for detecting near subsurface structures and soil heterogeneity that may be related to a variation in seismic shear (S)-wave velocity, (V_s). In general, the MASW method is divided into three major steps, namely, seismic data acquisitions in the field, dispersion analysis, and inversion of the dispersion curve images. By analyzing variations in S-wave velocity information on the material stiffness of the subsurface structure can be obtained. To produce a 2 dimensional (depth-distance) V_s map the procedure is generally as follows. First, multi-channel seismic records of surface waves are collected at a fixed location to determine a 1D (depth) shear wave velocity profile. Repeated recordings at points along a line provide multiple 1D profiles that can be combined to yield a 2D map.

One of the critical information of subsurface properties is the dispersion of Rayleigh surface waves in layered mediums. Most surface wave analysis methods are based on an accurate determination of the frequency-phase velocity ($f-c$)

Fig. 3 Samples of the collected raw data in the study area

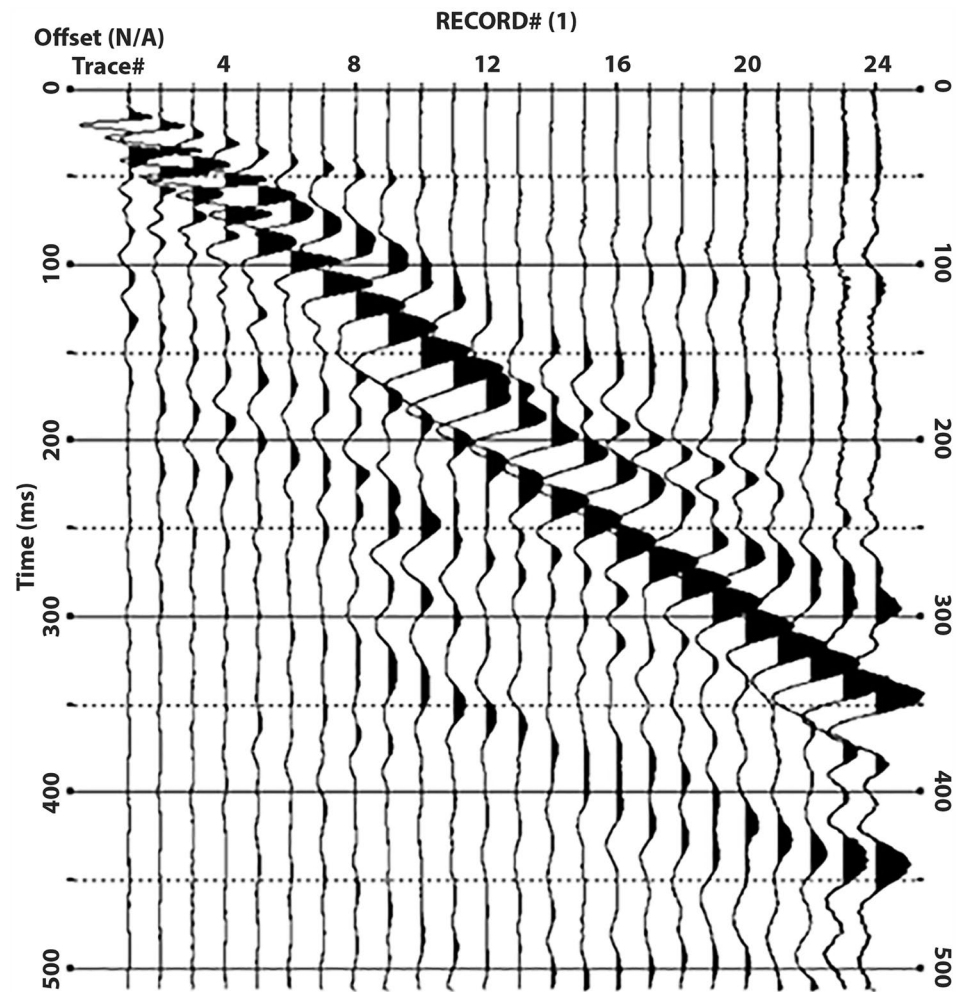
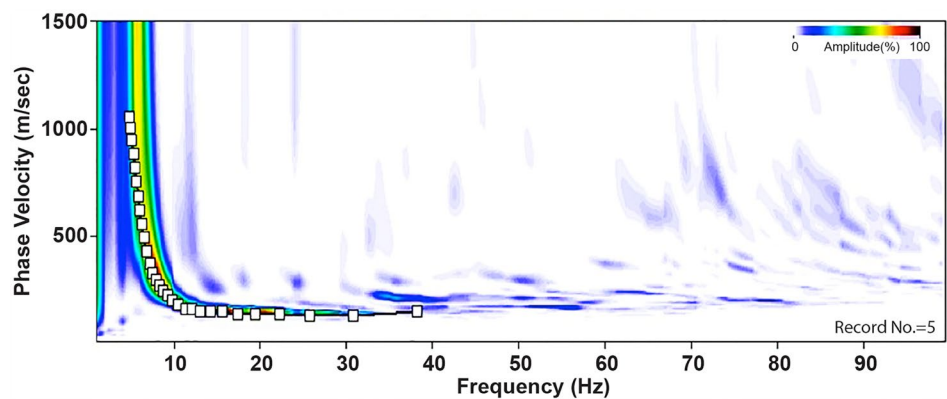


Fig. 4 Example of curve dispersion analysis from Serangai area. White rectangular boxes are dispersion curve extracted as input for the inversion step



of Rayleigh waves' fundamental mode (Park et al. 1997). Once the frequency-phase velocity (f - c) curve has been estimated from seismic traces, the V_s can be calculated through an inversion process, (Xia et al. 1999). The relation between Rayleigh surface wave velocity and the V_s depends on the mechanical properties of the medium, but typically the Rayleigh wave velocity is less than the V_s .

We conducted an active seismic survey at five locations, which are located in shoreline regions as shown in Fig. 2. In these surveys, we used a set of digital seismograph PASI 16S24, and recorded seismic waves from the vibration response of the underground surface. The seismic surface waves were recorded using 10 Hz vertical

Table 1 The average match observed and modeled of dispersion curves

Location	The average match (%)
Padang Betuah	82.76
Lais	81.14
Serangai	85.05
Ketahun	86.92
Seblat	81.92

geophones, and the seismic surface waves were generated with a sledgehammer.

We recorded the seismic surface waves with 24 geophones spaced at 2 m interval along a line following the trend of the shoreline, and the shot to the first geophone offset was 4 m. The MASW total record length was 512 ms with a sample interval of 125 μ s. We conducted 24 seismic wave recordings for each location to obtain the 2D subsurface structure. By putting together multiple 1D subsurface structural models obtained from sequentially collected seismic shot records along a seismic line, we were able to construct a 2D subsurface structure model. The geophones were moved 2 m at a time to create a total coverage along a distance of 94 m. For each every seismic record, at least three seismic data files were acquired and selection seismic data were carried out to obtain better the dispersion curve. This step was performed with extra care since several shots of seismic records contain noise from nearby ocean waves. ParkSeis seismic software was used to process the raw recordings. The 24-dispersion curves for each site location were extracted using field-based Rayleigh wave data, which supplied us with the best quality dispersion curves.

To obtain dispersion curves that have information of f - c curve, we used the Fast Fourier Transform (FFT) analysis. The frequency domain and phase velocity is controlled by the wave amplitude (A), the wave number (k), the geophone interval, the near offset and the energy source, respectively (Dikmen et al. 2010). Time scaling size for FFT was 1 s with a sampling rate of 1 ms which allows us to analyze frequencies up to 500 Hz. The space scaling size was 2 m. This number can improve the performance of the filtering. The frequency-domain band-pass filtering was applied. Cut-off limit for lowest frequency (0.1 Hz) and for highest frequency (50 Hz). After transforming the time-domain seismic data into a set of dispersion spectrums for each line using FFT, the dispersion curves are acquired by picking the energy peaks on the dispersion spectrum. On these spectrums, a set of points for the fundamental mode (M0) and for the higher modes (M1 to M4) can also identified. The selection can be made only for the modes clearly ascertainable from spectral analysis. Once we have a set of dispersion curves that consist of the frequency-phase velocity (f - c) curves, inversion was carried out automatically (Park et al. 1997; Xia et al. 1999).

4 Results and Discussion

For each location, there are 576 data (= 24 geophones \times 24 recordings). Figure 3 shows an example recording of seismic surface waves at the Serangai station. The arrival time and pulse shape of the seismic waves recorded at each geophone is displayed. Dispersion, in the form of the broadening of the wave pulse, and inhomogeneity (curvature in the line joining the peaks from one offset to the next) are evident. Some seismic traces data are noisy due to ocean wave action. Recordings were repeated in cases with high levels of noise to achieve good-quality seismic records.

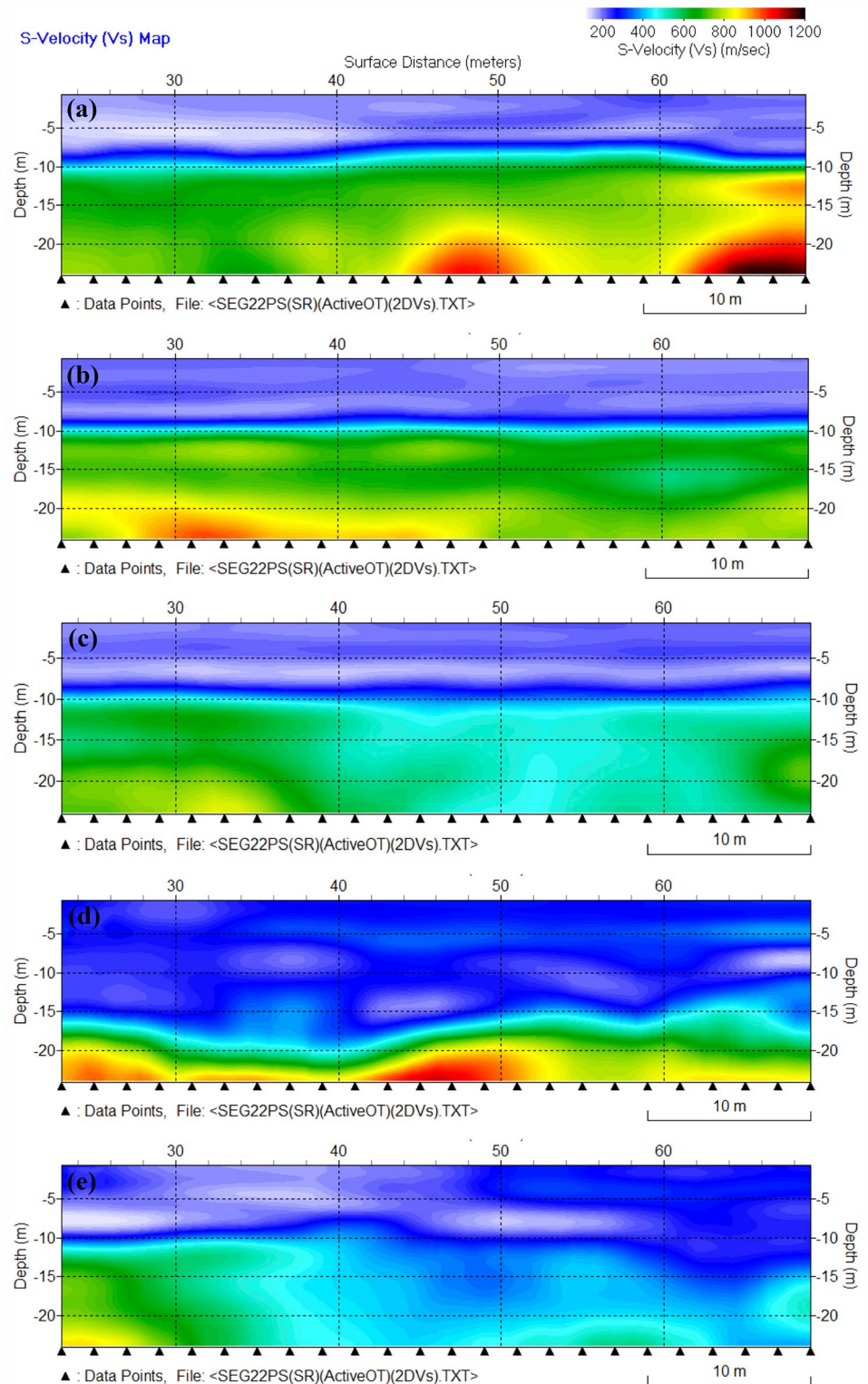
We picked high amplitudes of spectrum energy of seismic surface waves based on the percent value of spectrum energy. In this case, we concentrated on picking the dispersion curve from the f - c spectra that corresponded to the fundamental frequency, which is represented by the amplitude of spectrum energy of seismic surface waves.

Figure 4 shows an example of curve dispersion analysis from the Serangai station. As evident from Fig. 4, the lowest frequency components have high phase velocity and show stronger dependence on frequency than components in the higher frequency range. This makes the selection of the low-frequency part of the fundamental mode dispersion curve difficult to pick as an input for the inversion step.

To construct the 1D shear velocity profile, the selected dispersion curve (see boxes in Fig. 4) must be inverted. Inversion is generally a mathematically ill-posed problem in that a unique solution is not guaranteed. The fundamental mode (M0) generation algorithm (e.g. Schwab and Knopoff 1972) is robust and widely used, and has undergone many adjustments. Here, the inversion of the picked dispersion curves was carried out using the Levenberg–Marquardt least-squares algorithm proposed by Xia et al. (1999). Construction of the 2D profile interpolation of the 1D profiles is required. To select the best interpolation method for the 2D maps, we evaluated by calculating misfit between the observed dispersion curves and the modeled dispersion curves. Table 1 summaries the results and demonstrates that the match observed and modeled of dispersion curves that gave the best results.

Figure 5a–e shows the estimated 2D maps of V_s in Seblat, Ketahun, Serangai, Lais and Padang Betuah, respectively, from north to south. Depths are measured relative to the surface level a short distance landward from the cliff top. Positions for the datum at each site are shown as black vertical lines in Fig. 7. Figure 5 shows that the shear velocity profile extends to a depth of 25 m and suggests that the subsurface structure can be divided into a three-layer stratigraphy at most of the sites. A top layer with $V_s < 200$ m/s extending to a depth of about 10 m can be observed in Seblat, Ketahun and Serangai stations. However, at Lais and Padang Betuah,

Fig. 5. 2D subsurface structures at high-rate coastal abrasion areas in Northern Bengkulu using seismic MASW method at Seblat (a), Ketahun (b), Serangai (c), Lais (d) and Padang Betuah regions



the thickness of the top layer increases to a depth of about 15 m, which has $V_s < 300$ m/s.

The second major layer has V_s ranging from 600 to 800 m/s with depths of about 10–20 m that can be identified in Seblat, Ketahun and Serangai foreshore regions

(Fig. 5a–c). In the Lais foreshore region, the second stratigraphy layer extends from 15 to 22 m, whereas in Padang Petuah, it lies between 10 and 25 m. A third region, with $V_s > 800$ m/s, is also evident at all stations. This takes the form of a layer only at Lais, elsewhere it has the appearance

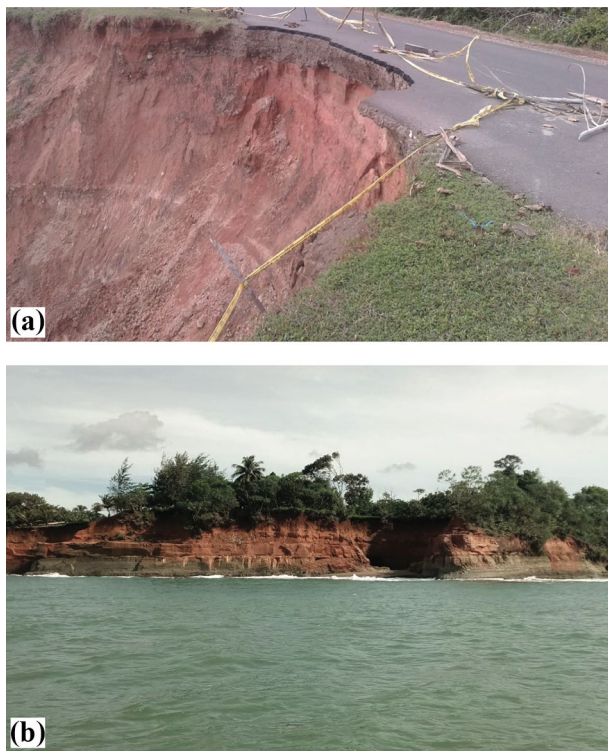


Fig. 6 Pictures of coastal erosion in the northern part of Bengkulu, **a** in Serangai shoreline area and **b** in Lais shoreline area

of an intrusion or dome. Between the main first and second layers is a narrow region with V_s values ranging from about 300–500 m/s. This region is well defined at Seblat, Ketahun and Serangai, whereas it is more undulating and diffuse at Lais and Pandang.

In top layer, the V_s value of < 300 m/s is typical of diluvial clay (Reynolds 2011; Foti et al. 2015), which is observed to characterize the topsoil (Fig. 5). We found a narrow region or ‘discontinuity layer’ between the first layer and the second layer with matching V_s values ranging from around 300 to 500 m/s, indicating that this region is probably made up of sand or silt, (see Reynolds 2011; Foti et al. 2015). The larger V_s value for the second layer, as compared to the first implies that the soil is saturated; with V_s ranging from about 600 to 800 m/s being consistent with this layer being composed of loose sand (Keceli, 2012). This finding matches well with in situ observations that we found in the field during seismic acquisition data (Fig. 6), where there is no lateral variation on substructure surface, which is also observed from the seismic image of 2D V_s values (Fig. 5).

Moreover, the last layer identified for Seblat, Ketahun and Lais foreshore regions occur at a depth of more than 20 m. The high values for V_s value at this layer imply that bedrock occurs at this depth. Based on an understanding of the area’s geology and the range of V_s for rock materials the bedrock is likely to be limestone according to Dal Moro

(2014) and Aziman et al. (2016). However, at Serangai and Padang Betuah foreshore regions, the higher shear velocities are absent suggesting a softer material than at Seblat, Ketahun and Lais foreshore regions.

Furthermore, we estimated the resolution of the models by reconstructing the input data. Overall, the resolution is very good from a depth of 3–15 m, which has a confidence level of 80–100%, meaning that the model can be trusted exactly. At a depth of 15–20, the average confidence level of 80% is good, while at depths > 20 m, the resolution is of medium confidence level. This is consistent with the arguments of Anukwu et al. (2018).

Figure 7a–e shows cross-sectional elevation transects at each of the sites corresponding to Fig. 5a–e, respectively. The intersect between the vertical black lines and the land elevation is the zero depth datum used in Fig. 5a–e. The MASW analysis lines are perpendicular to the elevation transects. The zero cliff height level corresponds to mean sea level. Figure 7g, h shows tidal recordings over the period January 2016–August 2020 at sites at each end of the study area. The records have very similar features indicating the tidal conditions do not alter significantly along the study shoreline. As can be seen the tidal range varies between ~0.5 m at neaps and ~1.5 m at spring tides, respectively, limiting the range of cliff face exposed to the sea. Bengkulu experiences a monsoonal climate; heavy monsoon storms tend to occur between October and April, with typical rainfall of 250 mm in October and November. These periods would coincide with wind-induced waves that might attack and abrade the toe of the cliffs. The western shore of Sumatra is protected against waves in the Indian Ocean by the Mentawai Ridge which rises sufficiently to form a string of islands approximately 100–200 km offshore.

Figure 7f shows a recording of waves during storm conditions in November 2018. The largest waves are about 3 m but are more typically about half that. With the modest tidal range, wave-driven erosion of the toe would be confined to a restricted region of the cliff face and manifest itself as scouring and notching. Little evidence of such processes is evident in the transects or photographs. This suggests that the observed cliff erosion may be more strongly associated with another mechanism, such as destabilization of the unsaturated layer due to high rainfall. The fact that the MASW results, together with the transect information, show the bottom of the unsaturated layer being close to the mean sea level is highly suggestive of rainfall being the main driver of cliff recession. The upper layer will absorb water from heavy monsoonal rains. The layer will eventually become saturated and form a slip plane. The weight of the saturated layer can cause the slip plane to slump.

With subsurface structure of a top layer of diluvial clay extending to between 10 and 15 m depth (Fig. 5), the cliffed

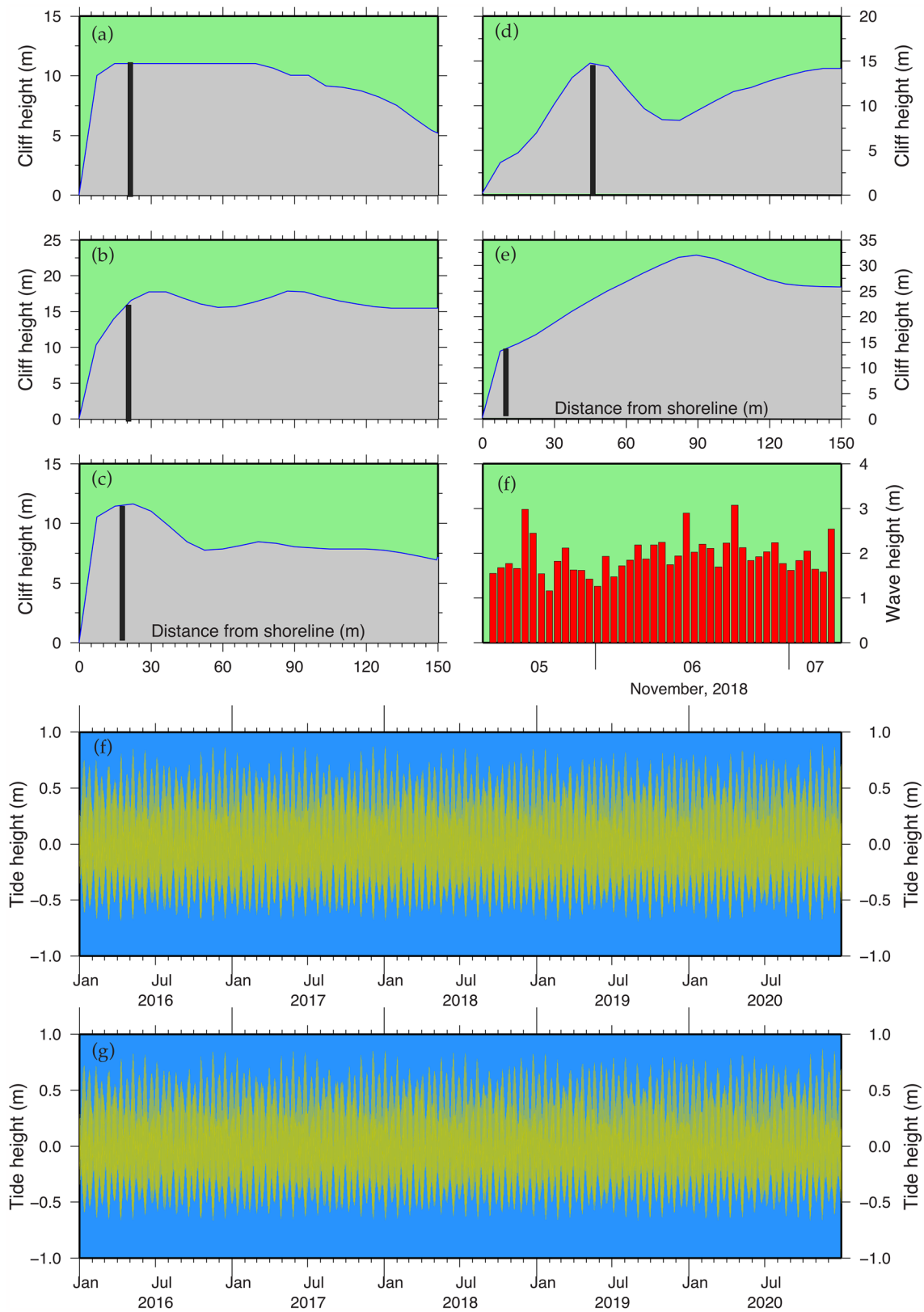


Fig. 7 The topography profile at Padang betuah (a), Lais (b), Serangai (c), ketahun (d) and Seblat respectively. Field observation of maximum height wave in November 2018 at Serangai region (f). Tide

gauge at Sebat station (f) and Pulau Baai (g), the nearest station to Padang Betuah site

coastal area of North Bengkulu is prone to instability after intense rainfall as water accumulating between the permeable and impermeable layers can lead to a loss of shear strength. The heavy rainfall distribution in North Bengkulu and the Central area of the Bengkulu Province, (Paski et al. 2021), can trigger cliff erosion. This is reflected by the total sediment flow in Bengkulu which reached 248.851 tons/year (Amri et al. 2017). In addition, Total Suspended Solid (TSS) levels in Bengkulu also exceeded water quality standards of 219.20 mm/dm³ during dry season and 175.75 mm/dm³ during rainy season, (Supriyono et al. 2019). The TTS value can be used as one indicator for causing the erosion in the environment despite the fact that this value may be influenced by runoff. The juxtaposition of weak geological structure, steep topography and high rainfall causes rapid erosion in the north Bengkulu area. In addition, based on Fig. 7, wave attack is not the main cause of cliff abrasion but makes it very vulnerable to erosion. This puts local communities and infrastructure at greater risk so that efforts to mitigate cliffed coastlines erosion and coastal damage are important.

5 Conclusion

We have investigated the subsurface structure of foreshores at high-rate coastal abrasion areas in northern Bengkulu using the 2D seismic MASW method. Based on our analyses, we conclude that in general the earth subsurface structure layer can be divided into three layers. The subsurface structure is composed predominantly of horizontally layered sedimentary materials with slight undulations. A top layer of diluvial clay, typical of the top soil, extends to between 10 and 15 m depth. This is separated from a second layer composed of loose saturated sand by a thin region comprising soft sand/silt. Below the second layer is a region of bedrock. This material is not in such a laminar alignment, adopting dome shapes and stronger undulating forms. From the values of shear wave velocity, we conclude that this bedrock is likely to be limestone. The protection afforded to the western Sumatran coast by the Mentawai Ridge together with the absence of scouring or notching of the cliff face suggests that wave attack is not the main cause of cliff abrasion. The high erodibility of the cliffs is related to the effects of heavy monsoonal rainfall, which saturates the upper layer of diluvial clay, thereby destabilising it.

We conclude that the combination of local geology and the region's propensity for intense rainfall make the shoreline in north Bengkulu very vulnerable to erosion. Wave action is thought unlikely to play a major role in causing cliff falls, but is sufficient to rework any fallen material along the shoreface. The steep morphology of the coastal bluff further contributes to the susceptibility of the shoreline to abrade.

Methods to stabilize the coast might include: stabilization of the cliff face; protection of the cliff toe through beach nourishment and/or armouring; reduction of the steepness of the coastal morphology through a combination of managed setback and sediment retention schemes.

Acknowledgements We would like to express our sincere gratitude to Research Center for Oceanography (P2O) Indonesian Institutes of Sciences (LIPI) for supporting this research. We also would like to thank students and technical staff from Physics Department, Bengkulu University for assisting with seismic data acquisitions during the field works. In particular, R Hanafi, who undertook UAV surveys of beaches in the study site. Tide gauge data at Sebat station and Pulau Baai station were obtained from <http://tides.big.go.id/> provided by Geospatial Information Agency of Indonesia.

Funding This study was funded by Demand Driven Research Grant (DDRG) through the Coral Reef Rehabilitation and Management Program-Coral Triangle Initiative (COREMAP-CTI) program (Grant Number B-1207/IPK.02/KS/III/2018).

Availability of Data and Materials Raw seismic data for this publication are available by personal request to asharm1@unib.ac.id.

Declarations

Conflict of Interest Authors declare that they do not have conflict interest and they also do not have any competing financial interests.

References

- Amri K, Barchia MF, Aprizal Y (2017) Analysis of erosion hazardous level and sedimentation in Manna Watershed, Bengkulu Province Indonesia. In: Sriwijaya International Conference on Engineering, Science and Technology, Pulau Bangka, Nov. 9–10, 2016, MATEC Web of Conferences, 101, 04002, <https://doi.org/10.1051/mateconf/201710104002>
- Anukwu G, Khalil A, Abdullah K (2018) Evaluating the effectiveness of the MASW technique in a geologically complex terrain. Paper presented at International Seminar on Mathematics and Physics in Sciences and Technology 2017. Batu Pahat, Malaysia, Oct. 28–29, 2017, Journal of Physics: Conference Series, 995, <https://doi.org/10.1088/1742-6596/995/1/012059>
- Ashton AD, Murray AB (2006) High-angle wave instability and emergent shoreline shapes: 1. Modeling of sand waves, flying spits, and capes. *J Geophys Res Earth Surf* 111(F4):314. <https://doi.org/10.1029/2005JF000422>
- Aziman M, Hazreek Z, Azhar A, Haimi D (2016) Compressive and shear wave velocity profiles using seismic refraction technique. Paper presented at the 4th International Conference on Science & Engineering in Mathematics, Chemistry and Physics 2016. Bali, Indonesia, Jan. 30–31, 2016, Journal of Physics: Conference Series, 710, <https://doi.org/10.1088/1742-6596/710/1/012011>
- Case M, Ardiansyah F, Spector E (2007) Climate change in Indonesia implications for humans and nature. World Wide Fund for Nature (wwf News) 1: 1–13. wwf.panda.org
- Chandran D, Anbazhagan P (2017) Subsurface profiling using integrated geophysical methods for 2D site response analysis in Bangalore city, India: a new approach. *J Geophys Eng* 14:1300–1314. <https://doi.org/10.1088/1742-2140/aa7bc4>

- Dal Moro G (2014) Surface wave analysis for near surface applications, 1st edn. Elsevier, p 252 (ISBN: 9780128007709)
- Daryono LR, Nakashima K, Kawasaki S, Suzuki K, Suyanto I, Rahmadi A (2020) Investigation of natural beachrock and physical-mechanical comparison with artificial beachrock induced by micp as a protective measure against beach erosion at Yogyakarta Indonesia. *Geosciences* 10(1):143
- Dickson ME, Walkden MJA, Hall JW (2007) Systemic impacts of climate change on an eroding coastal region over the twenty-first century. *Clim Change* 84:141–166. <https://doi.org/10.1007/s10584-006-9200-9>
- Dikmen U, Arısoy MO, Akkaya A (2010) Offset and linear spread geometry in the MASW method. *J Geophys Eng* 7:211–222. <https://doi.org/10.1088/1742-2132/7/2/S07>
- Eccleston P, Spyrou A (2019) Analysis of geophysical datasets for coastal vulnerability and asset management. *ASEG Ext Abstr* 1:1–3
- Foti S, Lai CG, Rix GJ, Strobbia C (2015) Surface wave methods for near-surface site characterization, 1st edn. CRC Press, Boca Raton, p 487 (ISBN 9781138077737)
- Hemer MA, Fan Y, Mori N, Semedo A, Wang XL (2013) Projected change in wave climate from a multimodel ensemble. *Nat Clim Change* 3:471–476
- Hussain Y, Cardenas-Soto M, Martino S, Moreira C, Borges W, Hamza O, Prado R, Uagoda R, Rodríguez-Rebolledo J, Silva RC, Martínez-Carvajal H (2019) Multiple geophysical techniques for investigation and monitoring of Sobradinho Landslide Brazil. *Sustainability* 11:6672. <https://doi.org/10.3390/su11236672>
- IPCC (2007) Climate change 2007: the physical science basis. In: Solomon S et al. (ed) Contribution of Working Group I to the Fourth Assessment Report of the Intergovernmental Panel on Climate Change. Cambridge University Press, Cambridge, New York
- Keceli A (2012) Soil parameters which can be determined with seismic velocities. *Jeofizik* 16:17–29
- Keskinsezer A, Dağ E (2019) Investigating of soil features and landslide risk in Western-Atakent (İstanbul) using resistivity MASW, Microtremor and Boreholes Methods. *Open Geosci* 11(1):1112–1128
- Lubis AM, Isezaki N, Sato T (2011) Two-dimensional coseismic deformation field of the Sumatra–Andaman earthquake 2004 M_w 9.2 derived from synthetic aperture radar observation. *Remote Sens Lett* 2(2):107–116
- Lubis AM, Hashima A, Sato T (2013) Analysis of afterslip distribution following the 2007 September 12 southern Sumatra earthquake using poroelastic and viscoelastic media. *Geophys J Int* 192(1):18–37
- Miller EB (2016) Seismic surface wave investigation of the Lake Erie Bluffs. *J Geogr Earth Sci* 4(2):11–30
- Mimura N (2013) Sea-level rise caused by climate change and its implications for society. *Proc Japan Acad Ser B Phys Biol Sci* 89(7):281–301. <https://doi.org/10.2183/pjab.89.281>
- Nicholls RJ, Leatherman SP (1995) The potential impacts of accelerated sea-level rise on developing countries. *J Coast Res* SI14:323
- Owoc B, Marciniak A, Dzierżek J, Kowalczyk S, Majdański M (2019) Seismic imaging of the mesozoic bedrock relief and geological structure under quaternary sediment cover: the Bolmin Syncline (SW Holy Cross Mountains, Poland). *Geosciences* 9:447. <https://doi.org/10.3390/geosciences9100447>
- Park CB, Miller RD, Xia J (1997) Summary report on surface-wave project at Kansas Geological Survey (KGS). Kansas Geological Survey, Lawrence, p 10
- Park CB, Miller RD, Xia J (1999) Multichannel analysis of surface waves. *Geophysics* 64:800–808
- Paski JAI, Permana DS, Alfuadi N, Handoyo MF, Nurrahmat MH, Makmur EES (2021) A multiscale analysis of the extreme rainfall triggering flood and landslide events over Bengkulu on 27th April 2019, The 9th National Physics Seminar 2020, AIP Conference Proceedings 2320, 040019-1-040019-8; <https://doi.org/10.1063/5.0037508>
- Rehman F, El-Hady SM, Atef AH, Harbi HM (2016) Multichannel analysis of surface waves (MASW) for seismic site characterization using 2D genetic algorithm at Bahrah area, Wadi Fatima Saudi Arabia. *Arab J Geosci* 9:519. <https://doi.org/10.1007/s12517-016-2544-1>
- Reynolds JM (2011) An introduction to applied and environmental geophysics. Wiley, West Sussex, p 710
- Samdara R (2014) Laju perubahan muka air laut di wilayah perairan pantai Bengkulu dengan menggunakan satellite Altimetry (Indonesian). *J Flux* 11:197–203
- Schwab FA, Knopoff L (1972) Fast surface wave and free mode computations. *Methods Comput Phys Adv Res Appl* 11:87–180. <https://doi.org/10.1016/B978-0-12-460811-5.50008-8>
- Supriyono S, Utaya S (2019) Study of quality changes and determination of water pollution index at river watershed Bengkulu Sumatra. *J Disaster Geogr Geogr Educ* 3(2):20–33. <https://doi.org/10.24036/sjdge.v2i1.136>
- Supriyono S, Utaya S, Taryana D, Handoyo B (2021) Spatial-temporal trend analysis of rainfall erosivity and erosivity density of tropical area in air Bengkulu Watershed Indonesia. *Quaestiones Geographicae* 40(3):125–142. <https://doi.org/10.2478/quageo-2021-0028>
- Toimil A, Camus P, Losada IJ, Le Cozannet G, Nicholls RJ, Idier D, Maspataud A (2020) Climate change-driven coastal erosion modelling in temperate sandy beaches: methods and uncertainty treatment. *Earth Sci Rev* 202:103110. <https://doi.org/10.1016/j.earsci.2020.103110>
- Türker U, Kabdaşlı MS (2006) The effects of sediment characteristics and wave height on shape-parameter for representing equilibrium beach profiles. *Ocean Eng* 33(2):281–291. <https://doi.org/10.1016/j.oceaneng.2004.12.016>
- Wang J, Church JA, Zhang X, Chen X (2021) Reconciling global mean and regional sea level change in projections and observations. *Nat Commun* 12(990):1–12. <https://doi.org/10.1038/s41467-021-21265-6>
- Warrick JA, Stevens AW, Miller IM, Harrison SR, Ritchie AC, Gelfenbaum G (2019) World's largest dam removal reverses coastal erosion. *Sci Rep* 9:13968. <https://doi.org/10.1038/s41598-019-50387-7>
- Xia J, Miller RD, Park CB (1999) Estimation of near-surface shear-wave velocity by inversion of Rayleigh waves. *Geophysics* 64:691–700